PHYSICAL REVIEW C VOLUME 45, NUMBER 4 APRIL 1992

Color transparency and high-energy $(p,2p)$ nuclear reactions

T.-S. H. Lee
Physics Division, Argonne National Laboratory, Argonne, Illinois 60439

G. A. Miller
Department of Physics FM-15, University of Washington, Seattle, Washington 98195
(Received 28 August 1991)

Predictions relevant for exploring color transparency in $(p,2p)$ nuclear reactions are often made by using simplified treatments of nuclear dynamics. We examine the extent to which the earlier predictions are valid by carrying out calculations using an improved treatment of the proton scattering wave functions, nucleon Fermi motion, and the effects of long- and short-range nuclear correlations. The consequences of two existing models of color transparency are also presented.

PACS number(s): 24.85.+p, 12.38.Aw, 12.38.Qk

I. INTRODUCTION

It has been suggested [1,2] that hadrons participating in high-momentum-transfer nuclear reactions undergo small initial- and final-state interactions with the nuclear medium. This unusual phenomenon, called color transparency, has generated much interest from theorists [3–10] and experimentalists [11–13], because it seems to be a testable prediction of quantum chromodynamics (QCD). The phenomenon is closely related to issues connected with the role of perturbative QCD in proton-proton scattering [14]. In this work we present predictions relevant for exploring color transparency in the semiexclusive $(p,2p)$ reaction on nuclei [15].

We begin by reviewing the arguments for observing color transparency of the $(p,2p)$ reaction. Consider nucleon-nucleon elastic scattering at large momentum transfer, where the amplitude is believed to be dominated by components of the nucleon wave function of small spatial extent. Each proton may be thought of as being a small colorless object just before or just after the high-momentum-transfer process takes place. The interaction cross section σ_{eff} for such a small colorless object with an ordinary nucleon is small because of the color screening effects of quantum chromodynamics. One way to test this interpretation is to consider the process in which the target nucleon is bound in a nucleus. The small size of σ_{eff} is manifest by the diminishing of initial- or final-state interactions as the beam energy increases. To understand the energy requirement, consider that a small component evolves into a nucleon of a standard size in a characteristic quark orbital time (τ_0 in the rest frame). At high energies time dilation effects increase this time to a value $\tau=\gamma\tau_0$. If τ is much longer than the time needed for the object to pass through the nucleus, the object can remain small while traveling the nucleus. In that case initial- or final-state interactions are expected to be small. Thus, at sufficiently high energies, the effects of color transparency should be observed and the semi-inclusive $(p,2p)$ reaction on nuclei is very close to the free pp elastic scattering averaged over the nuclear momentum distribution.

We shall be concerned with the following questions. How does this novel phenomenon emerge as the incident proton energy increases? What are the experimental signatures? The only published experiment seeking color transparency in the $(p,2p)$ reaction is that of Carroll *et al.* [11]. More accurate experiments are expected in the near future [12].

A rigorous QCD prediction of the $(p,2p)$ reaction seems inaccessible in the foreseeable future. But two complementary theoretical efforts can be used to explore and perhaps verify the existence of color transparency. First, it is necessary to establish the predictions expected in the absence of color screening effects. This requires the use of the best available nuclear theory. In particular, we need to know how the observables of interest [see Eqs. (11) and (12) below] are related to the well-established nuclear models. It is necessary to exclude the possibility that some observed features of the $(p,2p)$ reaction, unexpected in simplifying estimates, might simply be the manifestation of well-understood nuclear effects. Second, it is necessary to make a model with plausible assumptions, guided by QCD, for color transparency and thereby predict observables. For the $(p,2p)$ reaction this has been pursued by several groups [3,7,8,10]. In these exploratory attempts, the calculations were carried out with various simplifications of nuclear dynamics. It is necessary to reexamine the consequences of these models within well-established nuclear theory.

In this work we carry out the standard nuclear physics calculations of the $^{12}C(p,2p)$ reaction using the distorted-wave impulse approximation (DWIA). The terminology applies to calculations using the free nucleon-nucleon interaction to describe the process that knocks a bound proton out of the nucleus. Furthermore, the free proton-nucleon interaction is used to describe the proton-nucleus initial- and final-state interactions. Thus the incoming and outgoing protons are not plane waves, but are "distorted" by the interactions.

Our first objective is to present predictions for the observables that can be compared with the data of Carroll *et al.* [11] and could be relevant for planning experiments to be performed in the near future [12]. Our second objective is to examine the extent to which the simplifications used in earlier $(p,2p)$ calculations of color transparency are valid and provide more accurate comparisons with the standard nuclear physics predictions.

In Sec. II we present the DWIA formalism and establish the quantity of interest for exploring color transparency. The results and discussions are in Sec. III. A brief summary is presented in Sec. IV.

II. DWIA FORMULATION

It has been well established that the nuclear reactions at sufficient high energies can be described by the distorted-wave impulse approximation (see, for example, Refs. [16–18]). At GeV energies it is also known that the distorted waves can be calculated from the eikonal approximation [18].

In the DWIA the transition amplitude for the exclusive $(p,2p)$ reaction on nuclei can be written as

$$T_{f,i}=\sum_{\alpha}\langle f|b_\alpha|i\rangle\int d\mathbf{k}_1' d\mathbf{k}_2' d\mathbf{k}_1 d\mathbf{k}\,\delta(\mathbf{k}_1'+\mathbf{k}_2'-\mathbf{k}_1-\mathbf{k})\chi_{\mathbf{p}_1}^{(-)*}(\mathbf{k}_1')\chi_{\mathbf{p}_2}^{(-)*}(\mathbf{k}_2')t(\mathbf{k}_1',\mathbf{k}_2',\mathbf{k}_1,\mathbf{k},s_\alpha(\mathbf{p}_0,\mathbf{k}))\chi_{\mathbf{p}_0}^{(+)}(\mathbf{k}_1)\phi_\alpha(\mathbf{k})\ , \qquad (1)$$

where i and f denote, respectively, the initial nuclear state of A nucleons and the final nuclear state of $(A-1)$ nucleons. The nuclear structure information is described by the spectroscopic factor $\langle f|b_\alpha|i\rangle$ and single-particle wave function $\phi_\alpha(\mathbf{k})$, where α denotes the shell-model orbital of quantum numbers $(nljm)$. The spectroscopic factor is the amplitude that the removal of a proton from the initial state i leads to the final state f. The incoming and outgoing protons are described by the distorted waves $\chi_{\mathbf{p}}^{(\pm)}(\mathbf{k})$. The proton-proton (pp) transition amplitude t is evaluated at an invariant mass squared s_α, evaluated from the incident nucleon momentum $\mathbf{p}_0$, momentum $\mathbf{k}$ and energy of the struck nucleon in the target nucleus.

Expression (1) can be simplified when evaluated at high energies. First, we use the factorization approximation: The off-shell amplitude t in Eq. (1) is evaluated by approximating the momenta of the incoming and outgoing nucleons by their on-shell values

$$t(\mathbf{k}_1',\mathbf{k}_2',\mathbf{k}_1,\mathbf{k},s_\alpha(\mathbf{p}_0,\mathbf{k}))\rightarrow t(\mathbf{p}_1,\mathbf{p}_2,\mathbf{p}_0,\mathbf{k},s_\alpha(\mathbf{p}_0,\mathbf{k}))\ . \qquad (2a)$$

For our later discussions, it is useful to write down here the kinematic variables in the right-hand side of Eq. (2a). They are evaluated from the four-momentum p_α of the struck nucleon with a binding energy of ϵ_α in the nucleus,

$$p_\alpha\equiv(m-\epsilon_\alpha,\mathbf{k})\ , \qquad (2b)$$

and the four-momentum of the projectile,

$$p_0\equiv((m^2+\mathbf{p}_0^2)^{1/2},\mathbf{p}_0)\ . \qquad (2c)$$

Here m is the mass of the nucleon. The corresponding Mandelstam variables are

$$s_\alpha=(p_\alpha+p_0)^2\ , \qquad (2d)$$

$$t=(p_0-p_1)^2\ . \qquad (2e)$$

The distorted waves and single-particle wave function in coordinate space are defined by

$$\chi_{\mathbf{p}}^{(\pm)}(\mathbf{k})=\frac{1}{(2\pi)^{3/2}}\int e^{\pm i\mathbf{k}\cdot\mathbf{r}}\chi_{\mathbf{p}}^{(\pm)}(\mathbf{r})d\mathbf{r}\ , \qquad (3)$$

$$\phi_\alpha(\mathbf{k})=\frac{1}{(2\pi)^{3/2}}\int e^{+i\mathbf{k}\cdot\mathbf{r}}\phi_\alpha(\mathbf{r})d\mathbf{r}\ . \qquad (4)$$

Substituting Eqs. (2)–(4) into Eq. (1), we obtain

$$T_{f,i}=\sum_\alpha\langle f|b_\alpha|i\rangle\int d\mathbf{k}\ \delta(\mathbf{k}-(\mathbf{p}_1+\mathbf{p}_2-\mathbf{p}_0))F_\alpha(\mathbf{k})\times t(\mathbf{p}_1,\mathbf{p}_2,\mathbf{p}_0,\mathbf{k},s_\alpha(\mathbf{p}_0,\mathbf{k}))\ , \qquad (5)$$

with

$$F_\alpha(\mathbf{k})=(2\pi)^3\int d\mathbf{r}\ \chi_{\mathbf{p}_1}^{(-)*}(\mathbf{r})\chi_{\mathbf{p}_2}^{(-)*}(\mathbf{r})\chi_{\mathbf{p}_0}^{(+)}(\mathbf{r})\phi_\alpha(\mathbf{r})\ . \qquad (6)$$

Next, we employ the eikonal approximation to calculate the distorted waves from the nuclear density $\rho(\mathbf{r})$ and proton-nucleon total cross section σ^{tot}. The distorted wave of a given momentum $\mathbf{p}$ is expressed in terms of the longitudinal coordinate variable z_{p} and the impact parameter b_{p} defined by

$$\mathbf{r}=z_{\text{p}}\frac{\mathbf{p}}{|\mathbf{p}|}+\mathbf{b}_{\text{p}}\ , \qquad (7a)$$

with

$$z_{\text{p}}=\frac{\mathbf{r}\cdot\mathbf{p}}{|\mathbf{p}|}\ . \qquad (7b)$$

The distorted incoming wave is then of the following form:

$$\chi_{\mathbf{p}_0}^{(+)}(\mathbf{r})=\frac{1}{(2\pi)^{3/2}}e^{-i\mathbf{p}_0\cdot\mathbf{r}-A(\mathbf{r},\mathbf{p}_0)}\ , \qquad (8a)$$

with

$$A(\mathbf{r},\mathbf{p}_0)=\frac{\sigma^{\text{tot}}}{2}\int_{-\infty}^{z_{\mathbf{p}_0}}\rho(z',\mathbf{b}_{\mathbf{p}_0})dz'\ . \qquad (8b)$$

Similarly, we have, for the outgoing protons,

$$\chi_{\mathbf{p}_i}^{(-)*}(\mathbf{r})=\frac{1}{(2\pi)^{3/2}}e^{i\mathbf{p}_i\cdot\mathbf{r}-B(\mathbf{r},\mathbf{p}_i)}\ , \qquad (8c)$$

with

$$B(\mathbf{r},\mathbf{p}_i)=\frac{\sigma^{\mathrm{tot}}}{2}\int_{z_{\mathbf{p}_i}}^{\infty}\rho(z',\mathbf{b}_{\mathbf{p}_i})dz' , \tag{8d}$$

and $i=1,2$. We take σ^{tot} to be the total proton-nucleon cross section and use a value of 40 mb. The above formula can be used to obtain the scattering amplitude of the plane-wave impulse approximation (PWIA) by simply setting $\sigma^{\mathrm{tot}}=0$. Then the functions A and B vanish and the distorted waves $\chi^{(\pm)}$ reduce to plane waves. In the PWIA calculation, the initial- and final-state proton-nucleus interactions are therefore neglected.

One computes the cross section by taking the absolute square of $T_{f,i}$, multiplying by the appropriate phase space factors, and summing over the final states f that are allowed by conservation of four-momentum. We assume that the excitation energies of the states f is small compared to all other energies appearing in the phase-space factors. The neglect of the excitation energy allows us to use completeness (closure) to make the sum over all final states f. We stress that within this so-called closure approximation the dependence of the proton-nucleon transition matrix on the target nucleon momentum is retained. The collision invariant mass s_α for each single nucleon orbital α needs to be evaluated according to Eq. (2). This is an important feature of the present study since we are interested in the energy dependence of the $(p,2p)$ reaction and a careful treatment of the s dependence of the input proton-nucleon amplitude is essential.

By using the closure approximation [18] to sum over all final nuclear states f and nucleon spin variables, we then obtain the coincidence cross section of the semi-exclusive $(p,2p)$ reaction

$$\frac{d^3\sigma}{d\Omega_1 d\Omega_2 dp_1} =\int\sum_\alpha \frac{n_\alpha}{2l_\alpha+1}|F_\alpha(\mathbf{k})|^2\left[\frac{d\sigma^{pp}}{d\Omega}\right](s_\alpha,t)p_2^2dp_2d\mathbf{k} \times\delta(\mathbf{p}_1+\mathbf{p}_2-\mathbf{p}_0-\mathbf{k}) \times\delta(E(\mathbf{p}_1)+E(\mathbf{p}_2)-E(\mathbf{k})-E(\mathbf{p}_0)) , \tag{9a}$$

where $d\sigma^{pp}/d\Omega(s_\alpha,t)$ is the spin-averaged elementary pp differential cross section with s_α and t evaluated according to Eq. (2) and

$$n_\alpha=(2j_\alpha+1)^{1/2}\langle 0\|b_\alpha^\dagger b_\alpha\|0\rangle \tag{9b}$$

is the number of particles occupying the orbital α. The investigation of color transparency amounts to studying the relation between $d^3_\sigma/d\Omega_1 d\Omega_2 dp_1$ and the elementary pp cross section.

III. RESULTS AND DISCUSSIONS

We present calculations for experiments using in-plane symmetric kinematics $\theta_1=\theta_2=\theta$. That is, the momenta of the incident and outgoing protons are in the same plane (with proton 1 on the right and 2 on the left of the incident beam direction). For each incident proton energy, θ is chosen such that at the quasifree peak (the momentum of the struck nucleon $\mathbf{k}=0$) the scattering angle of the elementary pp scattering is 90° in the pp center-of-mass frame. This choice is made in order to compare our predictions with the data from Carroll *et al.* [11]. The calculated values of θ for the incident proton laboratory energies $E_{\mathrm{lab}}\le 40$ GeV are displayed in Fig. 1. Note that at very high energies θ is essentially constant at about 10°, but varies significantly in the region of the experiment of Carroll *et al.* [11]. In previous estimates [3,8,11] of transparency, this dependence is neglected by assuming $\theta_1=\theta_2=0°$. We will examine below how accurate this simplification is (see Fig. 5).

With the above choice of $(p,2p)$ kinematics, we can use the Ralston-Pire [5] parametrization of the 90° pp differential cross section. Normalizing their parametrization to the data [19], we find

$$\left.\frac{d\sigma}{dt}\right|_{\theta_{\mathrm{c.m.}}=90°}=16.51\ \mu\mathrm{b}\ (\mathrm{sr\ GeV}^2)^{-1} \times\left[\frac{11.303\ \mathrm{GeV}^2}{s}\right]^{10}f(s) , \tag{10}$$

where s and t are the pp Mandelstam variables and

$$f(s)=1+\rho_1\left[\frac{s}{\mathrm{GeV}^2}\right]^{1/2}\cos\phi(s)+\frac{\rho_1^2}{4}\frac{s}{\mathrm{GeV}^2} ,$$

with

$$\phi(s)=\frac{\pi}{0.06}\ln\{\ln[s/(0.01\ \mathrm{GeV}^2)]\}-2 ,$$

and $\rho_1=0.08$. The value of s is s_α as required by Eqs. (2) and (9).

It is important to note that the expression Eq. (10) varies as s^{-10} times a strongly oscillating function of s. The s^{-10} factor can be explained in terms of quark counting rules [20], but the QCD interpretation of the oscillating function $\theta(s)$ is much more complex [14]. Equation (10) provides a good description of the pp data and hence can be used in the present semiexclusive $(p,2p)$ calculation.

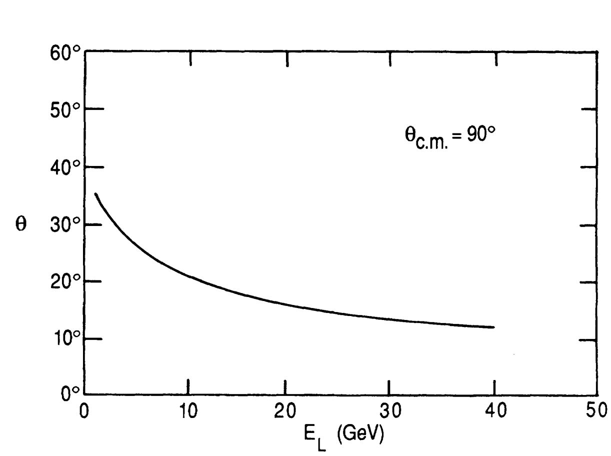

FIG. 1. Energy dependence of the $(p,2p)$ laboratory angles $\theta=\theta_1=\theta_2$ of symmetric kinematics, defined by 90° pp scattering in the pp center of mass.

We take the target nucleus to be ^{12}C, since targets are readily available and the nuclear wave function is well studied. Furthermore, the nucleus is large enough to represent a target of significant size, but small enough for detailed calculations to be performed in a reasonable amount of computer time. Our predictions for heavier nuclei and other scattering kinematics will be published elsewhere.

We first consider the simplest nuclear shell model for ^{12}C. The nucleons occupy the $\alpha = 0S_{1/2}, 1P_{3/2}$ orbitals, and the single-particle wave function $\phi_\alpha(\mathbf{r})$ is simply the harmonic-oscillator wave function (HOWF) with a size parameter $b = 1.64$ fm determined from electron scattering data. The occupation numbers [Eq. (9b)] are $n_{0S_{1/2}} = 2$ and $n_{1P_{3/2}} = 4$ since only protons contribute to the $(p,2p)$ knockout process.

The main features of the calculated $(p,2p)$ coincidence fivefold differential cross sections [Eq. (9)] can be illustrated by considering the knockout of the s-orbital protons. In the upper half of Fig. 2, we see that the distortion effects drastically reduce the magnitudes of the cross sections, but only slightly shift the positions of the peaks. The lower half of Fig. 2 shows the energy dependence of the DWIA results. As the energy increases, the peak's magnitude decreases and its position moves to a higher value of the detected proton momentum p_1.

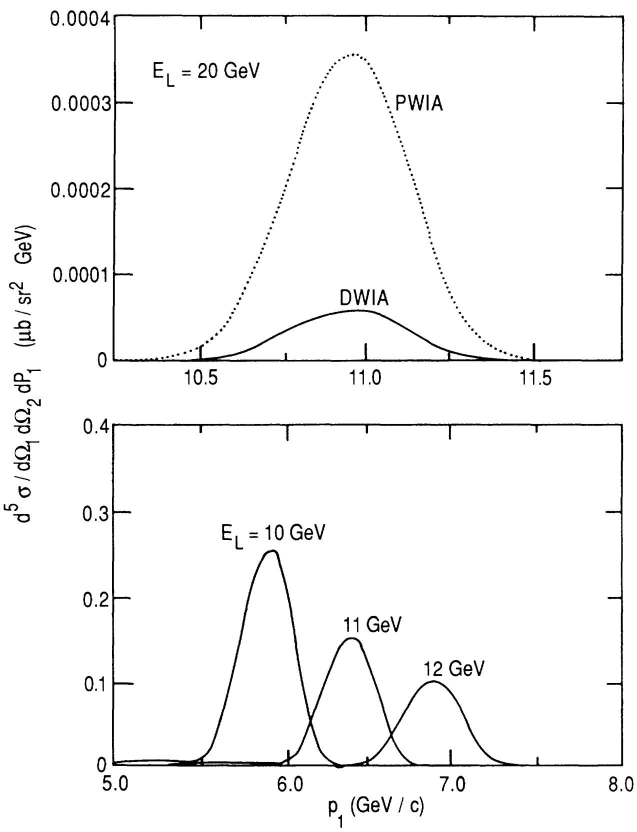

FIG. 2. ^{12}C$(p,2p)$ fivefold differential cross section for the knockout of a proton in the s orbital. The upper half shows the distortion effect at 20 GeV, and the lower half shows the energy dependence of the DWIA results.

Both the s- and p-orbital knockout are included in all of the following calculations. We will now focus on the differential cross section $d^2\sigma/d\Omega_1 d\Omega_2$, which is easier to measure. It is obtained by integrating the fivefold cross section [Eq. (9)] over the magnitude of the detected proton momentum p_1. Our DWIA and PWIA results for the scattering angles $\theta_1 = \theta_2 = \theta$ of Fig. 1 are shown in Fig. 3. This quantity of Fig. 3 is essentially the pp scattering at a fixed pp center-of-mass angle $\theta_{\text{c.m.}} = 90°$ that occurs in nuclei. Note that the Fermi motion of the bound nucleons causes the averaging of the elementary pp cross sections over a range of energies. The distortion effects reduce the magnitude of the differential cross section, but do not significantly change the energy dependence.

The quantity directly reflecting the difference between $(p,2p)$ on nuclei and free pp scattering is

$$T_{\text{direct}} = \frac{(d^2\sigma/d\Omega_1 d\Omega_2)(^{12}\text{C}(p,2p))|_{\text{DWIA},\theta}}{Z\ (d\sigma/d\Omega)(pp \to pp)|_{\theta_{\text{c.m.}}=90°}}\ , \qquad (11)$$

where the $(p,2p)$ scattering angles are $\theta_1 = \theta_2 = \theta$, displayed in Fig. 1. The elementary free pp cross section is evaluated from Eq. (10), and $Z = 6$ is number of protons in ^{12}C. Our result for T_{direct} is displayed in Fig. 4. Note that a very strong oscillatory structure is seen because the Fermi motion effects cause the numerator of Eq. (11) to be a smoother function of energy than the denominator.

From the theoretical point of view (taken by all of the current investigations of color transparency), the most interesting quantity is the nuclear effect after the effect of Fermi motion is removed. Therefore it is necessary to carefully assess the different possible procedures for treating Fermi motion effects. We proceed by following Ref. [11] to compute the following quantity:

$$T = \frac{(d^2\sigma/d\Omega_1 d\Omega_2)(^{12}\text{C}(p,2p))|_{\text{DWIA},\theta}}{(d^2\sigma/d\Omega_1 d\Omega_2)(^{12}\text{C}(p,2p))|_{\text{PWIA},\theta,\text{HOWF}(b=1.64\text{ fm})}}\ . \qquad (12)$$

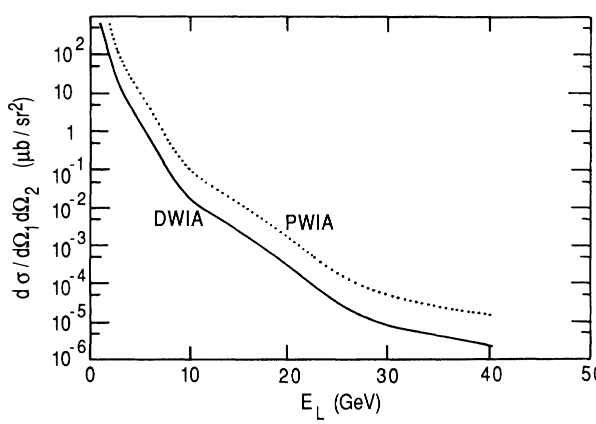

FIG. 3. Energy dependences of the ^{12}C$(p,2p)$ differential cross sections calculated from DWIA and PWIA.

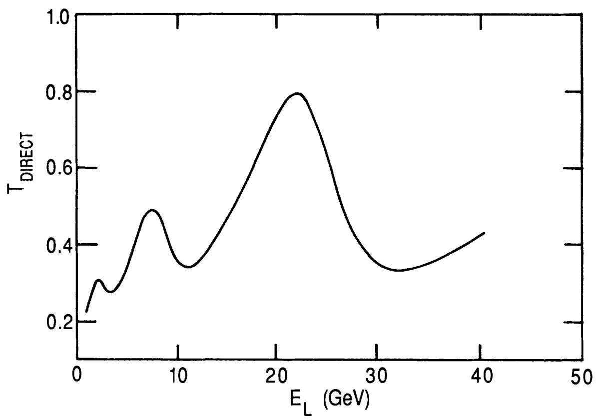

FIG. 4. Energy dependence of the transparency T_{direct} defined in Eq. (11).

The denominator of Eq. (12) is the PWIA result calculated by using the harmonic-oscillator wave function (HOWF) with a size parameter $b=1.64$ fm determined from electron scattering. In the simplest shell model, the DWIA calculation in the numerator is also calculated by using the same harmonic-oscillator wave function. The calculated transparency T is the solid curve in Fig. 5. We see that it is almost energy independent with very mild oscillations.

In the previous studies of color transparency [3,8], distortion effects are estimated by assuming that the outgoing protons are also in the direction of incident proton, i.e., neglecting the dependences of z_{p_i} and b_{p_i} on the directions of the outgoing protons [see Eq. (7)]. If we make the same approximation, we then obtain the dotted curves in Fig. 5. The differences between two results are about 10– 15% in the considered energy region. The use of such a forward-angle approximation, which drastically simplifies the numerical task, is therefore justified in estimating the transparency.

Clearly, our result shown in Fig. 5 is very different from the data of Carroll *et al.* It has been suggested that

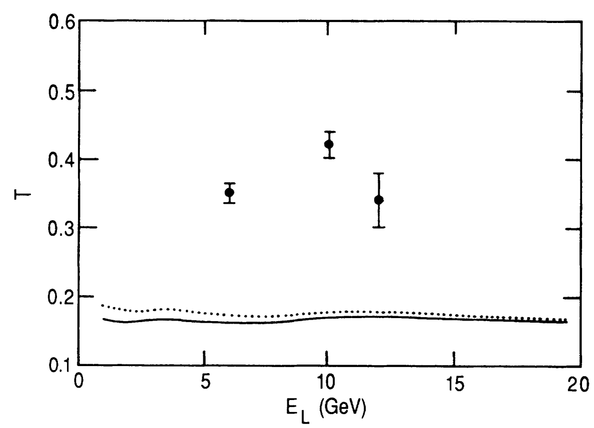

FIG. 5. Energy dependence of the transparency T defined in Eq. (12). The solid curve is the T computed with the scattering angles θ displayed in Fig. 1, and the dotted curve is obtained by using the approximation $\theta=0°$. The data are from Ref. [11]

such a large discrepancy can be removed if one assumes that a broad dibaryon resonance is excited and its propagation is strongly damped by the medium in the vicinity of resonance energy [4]. Another possibility is the Landshoff mechanism of Ref. [5], in which the ejected wave packet is a mixture of small- and large-sized objects. Detailed investigations [9] of both mechanisms show that each provides an improved agreement with the observations. However, neither effect is significant enough to reproduce the rapid energy variation of the data. The proposed more precise and higher-energy version of the Brookhaven National Laboratory experiment [12] is therefore of high interest.

Next, we investigate the effects of nuclear correlations which are beyond the description of the naive shell model with harmonic-oscillator wave functions. Extensive studies of nuclear low-lying states have provided us with information about nuclear correlations relevant for relatively large separations (≈ 1 fm) between nucleons. Thus we first consider this most well-known aspect of nuclear dynamics. The procedure is to include the configuration mixing caused by residual nucleon-nucleon interactions. Such interactions are determined by fitting nuclear spectra. We use the model of Cohen and Kurath [21] in which the nucleons in ^{12}C can also occupy the $1P_{1/2}$ orbital. The calculated occupation numbers are significantly different from that of the naive shell model and are $n_\alpha=2$, 3.27, and 0.73 for $\alpha=0S_{1/2}$, $1P_{3/2}$, and $1P_{1/2}$, respectively. The correlations also cause the single-particle wave function to differ from the simple harmonic-oscillator form. Following previous studies of reactions in which nucleons are knocked out of the nucleus, we use the wave functions generated from the well-established [22,23] density-dependent Hartree-Fock (DDHF) calculations. In Fig. 6 we compare these wave functions (solid curves) with that of the HOWF (dotted curves). Note that their differences at large values of r are most relevant to the present study, since $(p,2p)$ reactions mainly take place in the region near the nuclear surface.

When the two correlation effects considered above are included in the calculation, we obtain the solid curve in Fig. 7. Its difference with the dotted curve of the naive harmonic-oscillator shell-model prediction is mainly from the presence of 0.73 proton in the $1P_{1/2}$ orbital whose DDHF wave function is significantly different from the HOWF, as seen in Fig. 6. We have found that if the configuration mixing leads to significant occupations of higher orbitals, the calculated transparency will be very different from that of the naive harmonic-oscillator shell model. For example, we get a highly oscillating transparency if we assume that 25% of p-shell nucleons are moved to $2s$ orbital. The extensive studies of low-lying states of p-shell nuclei, however, rule out such a possibility. We emphasize that any attempt to consider nuclear correlations should be constrained by well-understood nuclear properties.

We now consider in more detail the dynamics of nucleon propagation in the nuclear medium. Repulsive short-range interactions prevent bound nucleons in nuclei from occupying the same spatial region. Thus a fast projectile, encountering a target proton, must move through an average distance of about 1 fm before encountering another. The calculation of the distortion effects defined by Eq. (8) neglects this nuclear granularity effect. The effects of these so-called short-range correlations can be approximately accounted for [25] by replacing the nuclear density function of ρ in Eq. (8) by

$$\rho(z',\mathbf{b}_p)\to\rho(z',\mathbf{b}_p)C(|z-z'|)\ , \tag{13}$$

where $C(u)$ is the correlation function. The value of z in the argument of the correlation function of Eq. (13) refers to either the upper [for Eq. (8b)] or lower [for Eq. (8d)] limit of integration. We use the nuclear matter estimate of Ref. [24] $C(u)=[g(u)]^{1/2}$ with

$$g(u)=\left[1-\frac{h(u)^2}{4}\right][1+f(u)]^2\ , \tag{14a}$$

where

$$h(u)=3\frac{j_1(k_F u)}{k_F u}\ , \tag{14b}$$

$$f(u)=-e^{-\alpha u^2}(1-\beta u^2)\ . \tag{14c}$$

The parameters for reproducing the nuclear matter correlation function are $\alpha=1.1$ and $\beta=0.68\ \mathrm{fm}^{-2}$. The Fermi momentum is chosen to be $k_F=1.36\ \mathrm{fm}^{-1}$. This simplified correlation function agrees well with ones derived from more detailed many-body calculations [25]. The transparency calculated from using Eqs. (13) and (14) to evaluate distorted waves [Eq. (8)] is the dotted curve in Fig. 8. We see that short-range correlation effects on nucleon propagation increase the predicted nuclear transparency. However, the energy dependence remains essentially unchanged.

The presence of short-range two-nucleon correlations also influences the nuclear wave function. It induces, for example, highly excited two-particle–two-hole components. If such components are large, the energy of the struck nucleon could be very different from the typical single-particle energies used in the present calculation. Such effects are discussed in Refs. [26]. However, the calculation including these higher-order effects requires a consistent improvement of the scattering formalism.

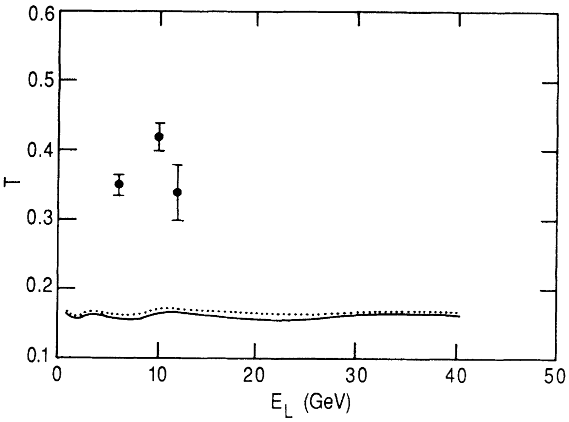

FIG. 7. Transparency T calculated from using DDHF wave functions (solid curve) is compared with that from using harmonic-oscillator wave functions (dotted curve). In both calculations the occupation numbers n_α of Cohen and Kurath [21] are used. The data are from Ref. [11].

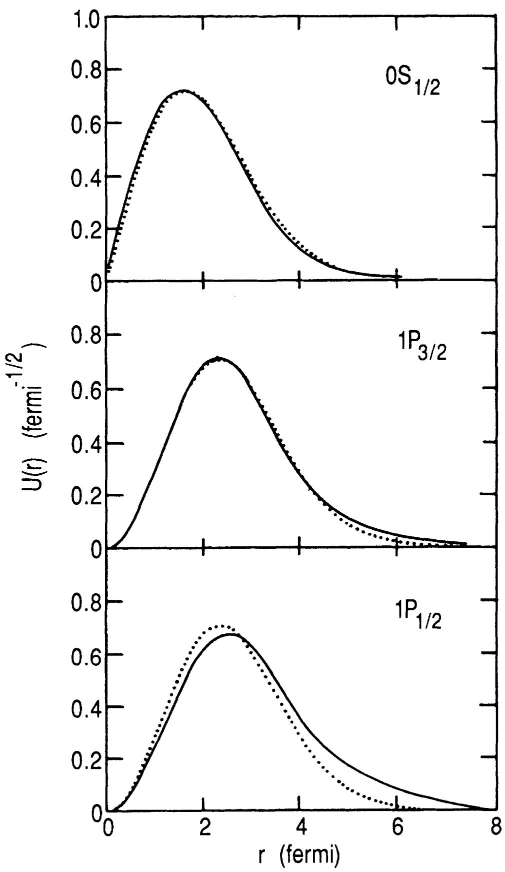

FIG. 6. Comparisons between the harmonic-oscillator wave functions (dotted curve) and DDHF wave functions (solid curve).

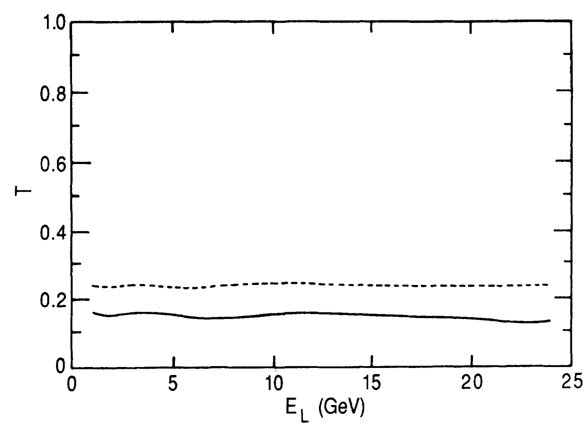

FIG. 8. Dotted (solid) curve is the transparency T calculated with the short-range correlation effects included (not included) in evaluating nucleon distortions.

This is certainly beyond the standard eikonal-DWIA approach adopted in this work.

Thus the standard eikonal DWIA predicts that the transparency T for $^{12}C(p,2p)$ [as defined in Eq. (12)] is fairly energy independent up to about 40 GeV incident proton energy. This means that future data showing a rise in T with the laboratory energy may be interpreted in terms of the novel QCD prediction of color transparency. To illustrate this possibility, we next present calculations including the effects of color transparency within our computational scheme. This is done by simply replacing the quantity σ^{tot} of Eqs. (8b) and (8d) by an effective cross section σ_{eff}. We consider the models of Ref. [3] (denoted by FLFS) and Ref. [8] (denoted by JM). In FLFS the effective cross section is given by

$$\sigma_{\mathrm{eff}}^{\mathrm{FLFS}}(z_{p_i},z') = \sigma^{\mathrm{tot}}\left\{\left[\frac{Z}{l_h}+\frac{\langle n^2k_t^2\rangle}{t}\left[1-\frac{Z}{l_h}\right]\right]\theta(l_h-Z) + \theta(Z-l_h)\right\}, \quad (15)$$

where $n=3$ and $Z=|z_{p_i}-z'|$. This expression is obtained by considering the most important energy denominator in perturbative QCD diagrams. $\langle k_t^2\rangle^{1/2}\approx 0.35$ GeV/c is the average transverse momentum of a parton in a hadron. The four-momentum transfer is t. The quantity l_h is the propagation distance at which an expanding hadron reaches its normal hadronic size: $l_h \simeq 2p/(0.7\ \mathrm{GeV}^2)$, where p is the momentum of the proton.

The effective cross section of JM is (in its simplest version)

$$\sigma_{\mathrm{eff}}^{\mathrm{JM}}(z_{p_i},z') = \sigma^{\mathrm{tot}}\left[1-\frac{p}{p_1}e^{i(p-p_1)Z}\right]. \quad (16)$$

In Eq. (16), p_1 is the momentum of a baryon resonance of a complex mass ($1444+75i$ MeV) produced at the same energy as the outgoing proton. This form is obtained by considering that the high-momentum-transfer process causes wave packets of small spatial extent to be produced. Such packets propagate as a sum of baryon resonances which interact with nucleons. The effective cross section of Eq. (16) arises by taking the coherent sum of the interactions. The small size of the packet leads to cancellations that cause

Using the functions σ_{eff} inside the integrals of (8b) and (8d) instead of the factor σ^{tot} leads to a calculation that includes the effects of color transparency. The results are compared with the standard nuclear physics DWIA result in Fig. 9. We regard the differences between the two models of color transparency as not very significant. Both treatments of color transparency yield curves in better agreement with the data than that of the standard DWIA. However, it is premature to declare that color transparency has been unambiguously discovered, before future high-accuracy experiments are performed.

It is useful to compare the present $(p,2p)$ results with

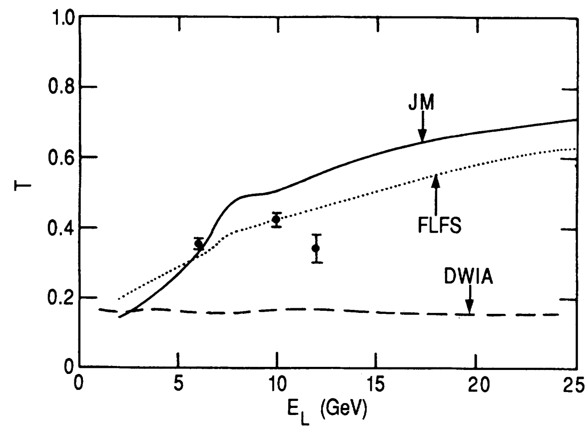

FIG. 9. Transparency T obtained with the effects of color transparency included. The solid curve is for the model of JM [8]; the dotted curve is for the model of FLFS [3]. The data are from Ref. [11].

existing calculations [3,8,9,25] of transparency in electron scattering. The major difference is that the computed values of the transparency are much smaller for the $(p,2p)$ than for the $(e,e'p)$ reaction. This is because the $(p,2p)$ reaction involves three distorted proton waves. However, there are some qualitative similarities between the two reactions. In both, the use of a standard distorted wave leads to a transparency that is independent of energy. The inclusion of color transparency effects leads to a transparency that rises with energy in both reactions. The $(p,2p)$ process is inherently the more complicated of the two reactions. This is because high-momentum-transfer process must convert each proton into a small-sized wave packet if color transparency is to occur. However, studies of both reactions will be needed if color transparency is to be verified and understood.

IV. SUMMARY

In this work we employ the distorted-wave impulse approximation and eikonal approximation to make predictions relevant to exploring color transparency in semiexclusive $(p,2p)$ reactions. Compared with the previous works [3,5,7,11], this work contains a significantly improved treatment of proton scattering waves and nuclear structure information. Evaluating the scattering amplitude with the correct $(p,2p)$ kinematics (instead of the usual forward scattering) changes the magnitude of the computed ratios of cross sections (transparency) by 10% or 15% (Fig. 5), but hardly changes the energy dependence. Including configuration mixing and using the density-dependent Hartree-Fock single-particle wave functions to compute the effects of nucleon motion lead to small differences with the calculations using a naive harmonic-oscillator shell model (Fig. 7). Including the effects of short-range correlations on proton propagation in nuclei changes the calculated transparency by about 30%, but does not change the energy dependence (Fig. 8). Thus our calculations verify the universal expectation that conventional mechanisms yield an almost energy-independent transparency. Our results incorporating the effects of color screening, displayed in Fig. 9, can be used in exploring color transparency in future more precise $(p,2p)$ experiments.

ACKNOWLEDGMENTS

This work was supported in part by the U.S. Department of Energy, Nuclear Physics Division, under Contracts No. W-31-109-ENG-38 and No. DE-FG06-88ER40427. The authors acknowledge many beneficial discussions held at the Institute for Nuclear Theory funded by the U.S. Department of Energy and the 1990 Argonne workshop on interfaces between nuclear and particle physics funded by the Argonne National Laboratory.

[1] A. H. Mueller, in *Proceedings of the Seventeenth Rencontre de Moriond, Moriond, 1982,* edited by J. Tran Thanh Van (Editions Frontières, Gif-sur-Yvette, France, 1982), p. 13.

[2] S. J. Brodsky, in *Proceedings of the Thirteenth International Symposium on Multiparticle Dynamics,* edited by W. Kittel, W. Metzger, and A. Stergiou (World Scientific, Singapore, 1982), p. 963.

[3] G. R. Farrar, H. Liu, L. L. Frankfurt, and M. I. Strikman, Phys. Rev. Lett. **61**, 686 (1988); **64**, 2996 (1990); Nucl. Phys. **B345**, 125 (1990).

[4] S. J. Brodsky and G. F. De Teramond, Phys. Rev. Lett. **60**, 1924 (1988).

[5] J. P. Ralston and B. Pire, Phys. Rev. Lett. **61**, 1823 (1988).

[6] J. P. Ralston and B. Pire, Phys. Rev. Lett. **65**, 2343 (1990).

[7] B. K. Jennings and G. A. Miller, Phys. Lett. B **236**, 209 (1990).

[8] B. K. Jennings and G. A. Miller, Phys. Rev. D **44**, 692 (1991).

[9] B. K. Jennings and G. A. Miller, TRIUMF-UWA report 1991 [Phys. Lett. B (submitted)].

[10] B. Z. Kopeliovich and B. G. Zakharov, Phys. Lett. B (to be published).

[11] A. S. Carroll *et al.*, Phys. Rev. Lett. **61**, 1698 (1988); S. Heppelmann, in *Nuclear Physics and the Light Cone,* edited by M. B. Johnson and L. S. Kisslinger (World Scientific, Singapore, 1989), p. 199.

[12] A. S. Carroll *et al.*, BNL experiment No. 850, 1991.

[13] R. Milner *et al.*, SLAC NE18 proposal, and private communications.

[14] J. Botts and G. Sterman, Nucl. Phys. **B325**, 62 (1989); J. Botts, *ibid.* **B353**, 20 (1991); J. Botts, J. Qiu, and G. Sterman, *ibid.* **A527**, 577c (1991); J. Botts and G. Sterman, Phys. Lett. B **224**, 201 (1989).

[15] The term "semiexclusive $(p,2p)$ reaction" refers to a nucleon knockout process which does not involve meson productions. This reaction can be measured only by an experiment which is able to reject events in which pions or heavier mesons are produced.

[16] N. S. Chant and P. G. Roos, Phys. Rev. **15**, 57 (1977), and other earlier references therein.

[17] P. G. Roos, L. Rees, and N. S. Chant, Phys. Rev. C **24**, 2647 (1981); P. Roos *et al.*, *ibid.* **38**, 2205 (1988).

[18] D. S. Koltun and J. M. Eisenberg, *Theory of Meson Interactions with Nuclei* (Wiley, New York, 1980).

[19] C. W. Akerlof *et al.*, Phys. Rev. **159**, 1138 (1967).

[20] D. Sivers, S. Brodsky, and R. Blankenbecler, Phys. Rep. C **23**, 1 (1976); A. Hendry, Phys. Rev. D **10**, 2030 (1974).

[21] S. Cohen and D. Kurath, Nucl. Phys. **A101**, 1 (1967).

[22] D. Vantherin and D. M. Brink, Phys. Rev. C **5**, 626 (1972).

[23] N. Van Gai and H. Sagawa, Phys. Lett. **106B**, 379 (1981); H. Sagawa, Prog. Theor. Phys. **S74**, 342 (1982).

[24] G. A. Miller and J. E. Spencer, Ann. Phys. (N.Y.) **100**, 562 (1976).

[25] O. Benhar, A. Fabrocini, S. Fantoni, G. A. Miller, V. R. Pandharipande, and I. Sick, Phys. Rev. C **44**, 2328 (1991).

[26] M. Strikman, Nucl. Phys. **A508**, 465c (1990); L. Frankfurt, M. Strikman, and M. B. Zhalov, Nucl. Phys. **A515**, 599 (1990); L. Frankfurt, G. A. Miller, and M. Strikman, Phys. Rev. Lett. **68**, 17 (1992).